

Electron-Phonon mechanism for Superconductivity in $\text{Na}_{0.35}\text{CoO}_2$: Valence-Band Suhl-Kondo effect Driven by Shear Phonons

Keiji YADA and Hiroshi KONTANI

Department of Physics, Nagoya University, Furo-cho, Nagoya 464-8602, Japan.

(Dated: May 24, 2019)

To study the possible mechanism of superconductivity in $\text{Na}_{0.35}\text{CoO}_2$, we examine the interaction between all the relevant optical phonons (breathing and shear phonons) and $t_{2g}(a_{1g} + e'_g)$ -electrons of Co-ions, and study the transition temperature for a s -wave superconductivity. The obtained T_c is very low when the e'_g -valence-bands are far below the Fermi level. However, T_c is strongly enhanced when the top of the e'_g -valence-bands is close to the Fermi level (say -50meV), thanks to interband hopping of Cooper pairs caused by shear phonons. This “valence-band Suhl-Kondo mechanism” due to shear phonons is significant to understand the superconductivity in $\text{Na}_{0.35}\text{CoO}_2$. By the same mechanism, the kink structure of the band-dispersion observed by ARPES, which indicates the strong mass-enhancement ($m^*/m \sim 3$) due to optical phonons, is also explained.

PACS numbers: 71.38.Cn, 74.20.-z, 74.25.Kc, 71.10.Fd

Despite enormous theoretical and experimental effort, the origin of superconductivity (SC) in $\text{Na}_{0.35}\text{CoO}_2 \cdot y\text{H}_2\text{O}$ ($T_c = 4.5\text{K}$) is still under controversial. Several NMR/NQR measurements above T_c have revealed the existence of prominent magnetic fluctuations with finite momenta [1, 2, 3], which might remind someone of unconventional SC due to Coulomb interactions. Below T_c , a sizable Knight shift is observed for both $\mathbf{H} \perp \mathbf{c}$ and $\mathbf{H} \parallel \mathbf{c}$, which indicates a singlet SC [4]. Whereas it is recognized only for $\mathbf{H} \perp \mathbf{c}$ by another group [5].

Significant information on the Fermi surface have been obtained by recent ARPES measurements: They show that $\text{Na}_{0.35}\text{CoO}_2(\cdot y\text{H}_2\text{O})$ possesses a single hole-like Fermi surface composed of a_{1g} -orbitals in Co-ions, whereas other two bands which originates from e'_g -orbitals are completely below the Fermi level [6, 7, 8]. They report that the top of e'_g -like valence-bands is located about $20 \sim 100\text{meV}$ below the Fermi level, irrespective that a LDA band calculation predicts the existence of Fermi surfaces of e'_g -bands, which are composed of six small hole pockets just inside of K points. [9]. Theoretically, absence of small hole pockets would be unfavorable for unconventional SC [10]. It is noteworthy that the “weak pseudo-gap behavior” observed in the uniform susceptibility below the room temperature in $\text{Na}_{0.35}\text{CoO}_2$ [1] is well reproduced by the fluctuation-exchange (FLEX) approximation only when small hole pockets are absent, as observed in ARPES measurements [11].

Besides the on-site Coulomb interaction, existence of strong electron-phonon interaction (EPI) in Na_xCoO_2 is indicated by various optical measurements [12, 13]. In addition, the quasiparticle dispersion for a_{1g} -band observed by ARPES measurement has a prominent “kink” structure around 70meV below the Fermi level, which is expected to originate from phonons because the energy of optical phonons is also $\sim 70\text{meV}$. The estimated mass-enhancement factor due to phonons is about three. On the other hand, the bandwidth of t_{2g} -bands observed by ARPES measurement is around 0.8eV , which is about

a half of the bandwidth given in the LDA band calculation [9]. Thus, the mass-enhancement factor due to Coulomb interaction is about two [14], so the total mass-enhancement factor becomes $2 \times 3 = 6$. This fact would indicate that the EPI will be dominant in Na_xCoO_2 .

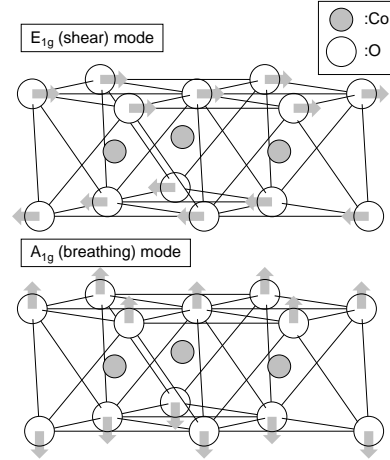


FIG. 1: The displacement of O-ions by E_{1g} (shear) mode and A_{1g} (breathing) mode.

In the present work, we analyzed the EPI based on the d - p model for $\text{Na}_{0.35}\text{CoO}_2$ given in ref.[11], and find that both shear and breathing optical phonons are strongly coupled with t_{2g} -electrons of Co-ions. If only the breathing phonon is taken into account, the T_c for s -wave SC obtained by the Eliashberg equation is very low. On the other hand, much higher T_c is obtained when we consider both shear and breathing phonons, thanks to the interband hopping of Cooper pair between the a_{1g} -conduction band and the e'_g -valence bands. This “valence-band Suhl-Kondo (SK) mechanism” due to shear phonons also gives a large mass-enhancement.

The structure of CoO_2 layer is a triangular network of edge sharing oxygen octahedra. The trigonal deformation of the octahedra splits the t_{2g} orbitals into a_{1g} or-

bital and twofold degenerate e'_g orbitals. Here we take the basis of t_{2g} electrons as $|a_{1g}\rangle = (|d_{xy}\rangle + |d_{yz}\rangle + |d_{zx}\rangle)/\sqrt{3}$, $|e'_g{}^1\rangle = (|d_{yz}\rangle - |d_{zx}\rangle)/\sqrt{2}$, and $|e'_g{}^2\rangle = (2|d_{xy}\rangle - |d_{yz}\rangle - |d_{zx}\rangle)/\sqrt{6}$. Here, we introduce V'_t to express the change of the crystalline electric splitting between a_{1g} and e'_g orbitals from the value given by the LDA band calculation [11]. V'_t decreases as the trigonal distortion is promoted.

First, we focus on the zone center phonon modes. NaCoO_2 has 7 kinds of irreducible representations for optical phonons per CoO_2 layer [15]. These phonons are separated into a soft group (3 modes) with frequencies below about 400 cm^{-1} and a hard group (4 modes) with frequencies between 450 and 650 cm^{-1} . The latter corresponds to CoO_2 octahedron's oscillating modes, which can give strong EPI. In these 4 modes, we find that only E_{1g} and A_{1g} modes strongly couple with t_{2g} electrons, whereas other two ungerade modes have no coupling with respect to the linear-displacement of oxygen ions. In E_{1g} and A_{1g} modes, oxygen ions oscillate in the direction parallel and perpendicular to CoO_2 layer, respectively, as shown in Fig. 1. Hereafter we call them "shear mode phonon" and "breathing mode phonon", respectively. Note that the shear mode belongs to a two dimensional representation.

Hereafter, we calculate the strength of the EPI via frozen phonon method. For that purpose, we ignore the effect of the trigonal distortion for the simplicity of calculation. The displacement due to m mode phonon ($m = BR, SH1, SH2$) is expressed as $\mathbf{u}_m = \sqrt{\frac{\hbar}{2M\omega_m}}(b_m + b_m^\dagger)$, where M is the mass of oxygen ion, ω_m is the frequency of oscillation and $b_m^{(\dagger)}$ is annihilation (creation) operator for phonon. The Hamiltonian which denotes EPI for multi-orbital model is written as follows.

$$H_{\text{EPI}} = \frac{1}{\sqrt{N}} \sum_m^{BR, SH1, 2} \sum_{\mathbf{k}, \mathbf{q}, \sigma} \hat{c}_{\mathbf{k}+\mathbf{q}\sigma}^\dagger \hat{V}^m \hat{c}_{\mathbf{k}\sigma} (b_{m,\mathbf{q}} + b_{m,-\mathbf{q}}^\dagger), \quad (1)$$

where $\hat{c}_{\mathbf{k}\sigma}^{(\dagger)} = (c_{\mathbf{k}, \alpha_{1g}, \sigma}^{(\dagger)}, c_{\mathbf{k}, \epsilon_g^1, \sigma}^{(\dagger)}, c_{\mathbf{k}, \epsilon_g^2, \sigma}^{(\dagger)})$ is annihilation (creation) operator's column (row) vector for electron, and \hat{V}^m is the coupling for m mode phonon. Hereafter, we drop the \mathbf{q} -dependence of \hat{V}^m and use the matrices for zone center phonon for the simplicity of calculation.

By choosing an appropriate coordinate axis for shear phonons, the matrices have the following form[16].

$$\hat{V}^{BR} = \begin{pmatrix} a_1 & 0 & 0 \\ 0 & a_2 & 0 \\ 0 & 0 & a_2 \end{pmatrix}, \quad (2)$$

$$\hat{V}^{SH1} = \begin{pmatrix} 0 & b_1 & 0 \\ b_1 & 0 & -b_2 \\ 0 & -b_2 & 0 \end{pmatrix}, \quad \hat{V}^{SH2} = \begin{pmatrix} 0 & 0 & -b_1 \\ 0 & b_2 & 0 \\ -b_1 & 0 & -b_2 \end{pmatrix}. \quad (3)$$

First, we consider the EPI originates from the change of the Coulomb potential for t_{2g} electrons due to the

displacement of oxygen ions, by considering oxygen ions as point charges. The obtained result is $a_1^C = -C(1 - \frac{4}{7}\frac{r_d^2}{a^2})$, $a_2^C = -C(1 + \frac{2}{7}\frac{r_d^2}{a^2})$, $b_1^C = C\frac{2}{7}\frac{r_d^2}{a^2}$, $b_2^C = \frac{1}{4\sqrt{2}}b_1^C$ on the order of a^{-4} [16]. Here a is the lattice constant between Co site and oxygen site, r_d is the ionic radius of Co^{3+} , and $C = \frac{2e^2}{a^2} \sqrt{\frac{\hbar}{2M\omega_m}} \cdot 2\sqrt{3}$; $\sqrt{\frac{\hbar}{2M\omega_m}} = 0.043\text{\AA}$ if we put $\omega = 60 \text{ meV}$. By using the values $a \approx 1.9\text{\AA}$ and $r_d \approx 0.61\text{\AA}$, C is estimated to be 0.87 eV .

Next, we consider the EPI originated from the change of the transfer integrals between Co and O. According to the Harrison's law ($t \propto a^{-4}$)[17], $\delta t_{pd\pi} = -t_{pd\pi} \frac{4}{a} \mathbf{u}_m \cdot \mathbf{e}_{\text{O-Co}}$, where $\mathbf{e}_{\text{O-Co}} = (\mathbf{r}_\text{O} - \mathbf{r}_\text{Co})/a$. The $2p$ orbitals of oxygen are filled with electrons. When we consider the virtual process where a *hole* of t_{2g} orbitals transfers to $2p$ orbitals and turns back, its energy shifts by $-\frac{t_{pd\pi}^2}{\Delta_{pd}}$ per one oxygen ion, where Δ_{pd} is charge transfer energy. So the variation of the *electron* level accompanied by the change of $t_{pd\pi}$ is $\delta \varepsilon_d = \frac{2t_{pd\pi} \delta t_{pd\pi}}{\Delta_{pd}}$. Up to the fourth order processes, we obtain $a_1^T = a_2^T = -2T$, $b_1^T = T$, $b_2^T = T/\sqrt{2}$, where T is given by

$$\frac{16}{\sqrt{3}} \frac{t_{pd\pi}^2}{\Delta_{pd}} \frac{1}{a} \sqrt{\frac{\hbar}{2M\omega_m}} \left\{ 1 + \frac{1}{\Delta_{pd}} (|t_{pp\sigma}| + |t_{pp\pi}|) + \frac{1}{\Delta_{pd}^2} \left(\frac{17}{4} t_{pp\sigma}^2 + \frac{29}{4} t_{pp\pi}^2 + \frac{9}{2} |t_{pp\sigma} t_{pp\pi}| + \frac{t_{pd\pi}^2 n_d}{6} \right) \right\}.$$

Here, we considered only nearest neighbor hoppings between Co-O and O-O. Using the values of Slater-Koster parameters given in [11], T is estimated to be 0.158 eV .

Thus, we obtain $b_1 = b_1^C + b_1^T = 0.21$, $b_2 = b_2^C + b_2^T = 0.12$ for shear phonons. As regards breathing phonon, we need to consider the chemical potential shift $\delta\mu$ caused by the A_{1g} frozen phonon since $\text{Tr}\{\hat{V}^{BR}\}$ is finite as shown eq.(2). Because of the conservation of electron number, $\rho_d(0)(\delta\varepsilon_d + \delta\mu) + \rho_p(0)\delta\mu = 0$, where $\rho_d(0)$ and $\rho_p(0)$ are the DOS of d-electrons and p-electrons at Fermi level. So effective shift of $3d$ level is $\delta\tilde{\varepsilon}_d = \delta\varepsilon_d + \delta\mu = \frac{\rho_p(0)}{\rho_d(0) + \rho_p(0)} \delta\varepsilon_d$. According to the band calculation[9] or in the present tight-binding model, $\frac{\rho_p(0)}{\rho_d(0) + \rho_p(0)} \sim 0.2$.

In conclusion, $a_1 = 0.2(a_1^C + a_1^T) \sim -0.2 \approx a_2$. Note that such a screening effect due to $\delta\mu$ is absent for shear phonons, so the estimated values of b_1 and b_2 are reliable.

In what follows we analyze the strong-coupling Eliashberg equation numerically. According to first-principle linear response calculation[15], frequencies of shear and breathing phonons are about 500 cm^{-1} and 600 cm^{-1} , respectively, and they are almost dispersionless. To reduce the number of model parameters to simplify the analysis, we take $\omega_D = 550 \text{ cm}^{-1} \sim 68.2 \text{ meV}$ for both phonons. In the present numerical calculation, we put

$$a_1 = 2a_2 = -\alpha^{BR}, \quad b_1 = 4\sqrt{2}b_2 = \alpha^{SH}. \quad (4)$$

We assume $\alpha^{BR} = \alpha^{SH} = 0.2$ considering that the estimated values of a_1 and b_1 are about 0.2 . Both a_1 and b_1

are important parameters for the SC because they are related to a_{1g} -orbital which makes the large Fermi surface around the Γ point. Whereas a_2 and b_2 are less important when small hole-pockets composed of e'_g orbitals are absent. We use one-loop approximation to calculate the self-energy $\Sigma(i\omega_n)$.

$$D(i\omega_n) = \frac{2\omega_D}{\omega_D^2 + \omega_n^2}, \quad (5)$$

$$\hat{\Sigma}(i\varepsilon_n) = \frac{T}{N} \sum_{\mathbf{k}, n', m} \hat{V}^m \hat{G}(\mathbf{k}, i\varepsilon_n - i\omega_{n'}) \hat{V}^m D(i\omega_{n'}), \quad (6)$$

$$\hat{G}(\mathbf{k}, i\varepsilon_n) = \left(\left(\hat{G}^{(0)}(\mathbf{k}, i\varepsilon_n) \right)^{-1} - \hat{\Sigma}(i\varepsilon_n) \right)^{-1}, \quad (7)$$

where $\omega_n = 2n\pi T$, $\varepsilon_n = (2n+1)\pi T$. These equations are solved self-consistently.

Figure 2 shows the V'_t -dependence of the inverse of the renormalization factor (or the mass-renormalization factor) $z_\ell^{-1} = 1 - \frac{\partial}{\partial \omega} \Sigma_\ell(\omega) \Big|_{\omega \rightarrow 0}$ at $T = 0.005$ (eV), where Σ_ℓ is the normal self-energy for ℓ orbital. We have checked that z_ℓ^{-1} is almost invariant against the temperature in the present calculation. At $(\alpha^{SH}, \alpha^{BR}) = (0.2, 0.2)$, z_ℓ^{-1} for a_{1g} orbital decreases as V'_t increases. Note that e'_g -band is completely below the Fermi level for $V'_t > 0.06$. To investigate the role of two kind of phonons, we perform the calculation for $(\alpha^{SH}, \alpha^{BR}) = (0, 0.2)$ and $(\alpha^{SH}, \alpha^{BR}) = (0.2, 0)$ for comparison. At $V'_t = 0.06$ where top of e'_g -band is just at the Fermi level, about 65% of the mass-enhancement for a_{1g} -band is brought by shear phonons which mediate the inter-band process, and its ratio gradually decreases as V'_t increases.

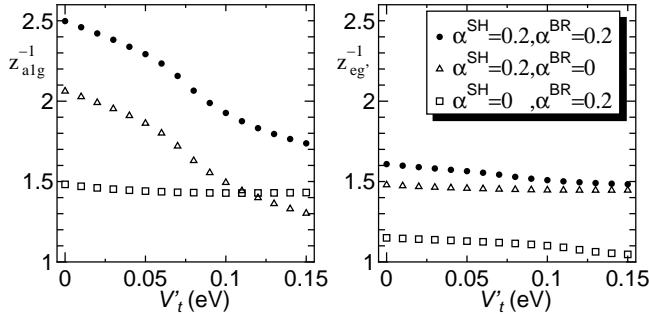


FIG. 2: Obtained z_ℓ^{-1} for a_{1g} (left) and e'_g (right) orbital.

Figure 3 is the renormalized band structure $E_{\mathbf{k}}^*$ for Γ -K direction in the Brillouin zone obtained by $\det[\hat{G}^{R-1}(E_{\mathbf{k}}^*) + \hat{G}^{A-1}(E_{\mathbf{k}}^*)] = 0$. At $|E_{\mathbf{k}}^*| \lesssim \omega_D$, the electronic band is renormalized significantly and kink structure appears in the a_{1g} band. This kink structure agrees well with the observation by ARPES measurements[6]. The e'_g band is also renormalized by phonon, and its upper side has a flattened structure for $|E_{\mathbf{k}}^*| \lesssim \omega_D$. The inset shows the top of e'_g band measured from the Fermi level, Δ , which is different from the original value without interaction. The small pockets disappears at $V'_t \simeq 0.1$

without interaction [11], but they disappear at $V'_t \simeq 0.06$ when the EPI is taken into account. This boundary value of V'_t does not change even if only shear phonons are into account, which means that the shear phonons depress the e'_g band to lower energy due to the off-diagonal elements of the self-energy. Although there is a linearity between Δ and V'_t , its gradient changes at $V'_t \simeq 0.06$ (eV) where the top of the e'_g band just cross the Fermi level. We comment that the second kink structure around $2\omega_D$ is a famous artifact of dispersionless Einstein phonon, so it will disappear when more realistic optical phonons with small dispersions are assumed.

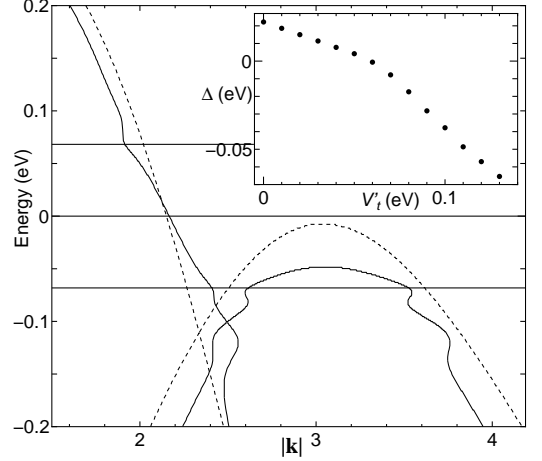


FIG. 3: The renormalized band structure $E_{\mathbf{k}}^*$ (solid line) for Γ -K direction and the original band structure $\varepsilon_{\mathbf{k}}$ (dashed line) of tight-binding model at $V'_t = 0.11$ (eV). Inset shows the V'_t -dependence of the top of the e'_g band, Δ .

Here, T_c is decided on condition that the eigenvalue of the Eliashberg equation, λ , is equal to one:

$$\lambda \hat{\phi}(i\varepsilon_n) = \frac{T}{N} \sum_{\mathbf{k}, n', m} \hat{V}^m \hat{G}(\mathbf{k}, i\varepsilon_{n'}) \hat{\phi}(i\varepsilon_{n'}) \times \hat{G}(-\mathbf{k}, -i\varepsilon_{n'}) \hat{V}^m D(i\varepsilon_n - i\varepsilon_{n'}), \quad (8)$$

here we assumed a \mathbf{k} -independent gap function $\hat{\phi}(i\varepsilon_n)$. Figure 4 shows the V'_t -dependence of T_c . At $(\alpha^{SH}, \alpha^{BR}) = (0.2, 0.2)$, T_c increases as V'_t decreases, whose change is much faster than the mass-renormalization factor does. The obtained T_c is high when the small pockets of e'_g band are present ($V'_t \lesssim 0.06$). However, it is noteworthy that T_c keeps high values for a while even after small pockets disappear, irrespective of the fact that the DOS suddenly decreases by one-third at $V'_t = 0.06$ (eV). To find out the reason, we study the case of $(\alpha^{SH}, \alpha^{BR}) = (0, 0.2)$ and $(\alpha^{SH}, \alpha^{BR}) = (0.2, 0)$ for comparison. In the former case, T_c is low and it is independent of V'_t . In the latter case, T_c drops quickly when the small pockets disappear because shear phonons do not produce the attractive force between a_{1g} electrons. The reduction of T_c for $(\alpha^{SH}, \alpha^{BR}) = (0.2, 0.2)$ is slower than the case of

$(\alpha^{SH}, \alpha^{BR}) = (0.2, 0)$, and T_c is considerably higher than that for $(\alpha^{SH}, \alpha^{BR}) = (0, 0.2)$ even when the small pockets disappear. It is understood that the shear phonons support the SC and raise T_c for wide range of V'_t . Because the shear phonons enable cooper pairs to transit from a_{1g} orbital to e'_g orbital, a sort of SK mechanism works and T_c increases. Indeed, the gap function $\phi_\ell(\omega)$ is finite only for a_{1g} band for $(\alpha^{SH}, \alpha^{BR}) = (0, 0.2)$ for $V'_t > 0.06$, on the contrary, $\phi_\ell(\omega)$ is finite for both a_{1g} and e'_g bands when $(\alpha^{SH}, \alpha^{BR}) = (0.2, 0.2)$. By the analytical study for $T_c \ll -\Delta \ll \omega_D$ [16], we derive that $T_c \approx \omega_D \exp(-1/\lambda_{\text{eff}}^*)$, where λ_{eff}^* is given by

$$\lambda_{\text{eff}}^* = \lambda_1^* + \frac{2\lambda_2^*\lambda_3^*\{\frac{1}{2}\log(\frac{\omega_D}{|\Delta|}) + \frac{1}{\pi}\}}{1 - \lambda_4^*\{\frac{1}{2}\log(\frac{\omega_D}{|\Delta|}) + \frac{1}{\pi}\}} \quad (9)$$

where $\lambda_1^* = \frac{2a_1^2}{\omega_D} z_{a_{1g}} \rho_{a_{1g}}$, $\lambda_2^* = \frac{2b_1^2}{\omega_D} z_{a_{1g}} \rho_{a_{1g}}$, $\lambda_3^* = \frac{2b_2^2}{\omega_D} z_{e'_g} \rho_{e'_g}$, $\lambda_4^* = \frac{2a_2^2}{\omega_D} z_{e'_g} \rho_{e'_g}$. In the derivation of Eq.(9), we put $b_2 = 0$ and we simplified the DOS as $\rho_{a_{1g}}(\omega) = \rho_{a_{1g}}$ and $\rho_{e'_g}(\omega) = \rho_{e'_g} \theta(\Delta - \omega)$ per orbital. When $|\Delta| \lesssim \omega_D$, the second term raises λ_{eff}^* and T_c . When $|\Delta|/\omega_D = 1/4$ ($V'_t \simeq 0.09$), $\frac{1}{2}\log(\frac{\omega_D}{|\Delta|}) + \frac{1}{\pi} \simeq 1$, and we estimate that $\lambda_1^* = \lambda_2^* \approx 0.25$, $\lambda_3^* \approx 0.50$, $\lambda_4^* \approx 0.126$ in the present model. Thus, λ_{eff}^* increases by 0.32 to 0.57 due to the second term, which is recognized as the valence-band SK effect.

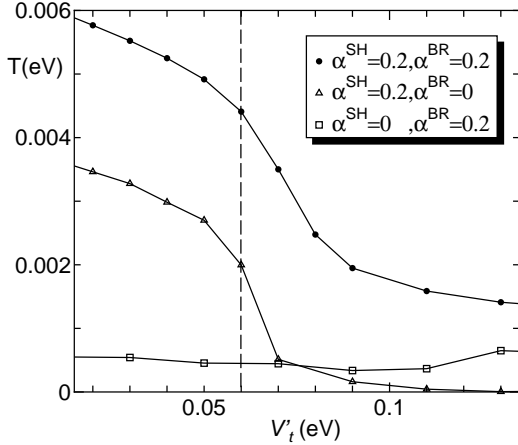


FIG. 4: V'_t -dependence of the critical temperature T_c .

Finally, we comment on the possible origin of the anisotropy of the superconducting gap, which is suggested by the absence of the coherence peak and by the specific heat measurement below T_c . We expect that an anisotropic s -wave state is realized due to the strong anti-ferromagnetic fluctuations, as realized in boron carbide, (Y,Lu)Ni₂B₂C [18]. This is an important future problem. We also comment that the effect of hydration on T_c . Figure 4 tells that the reduction of V'_t due to hydration [19] would explain why only hydrated samples show SC. We stress that the e'_g -band in Na_{0.35}CoO₂ · yH₂O does not intersect the Fermi level because the electronic heat coefficient γ is almost unchanged by hydration [1]. Otherwise, γ should increase to more than three times the experimental value by hydration, according to the change of the DOS at the Fermi level [11]. We comment that ref.[20] proposes a mechanism of s -wave SC due to the long-range Coulomb interactions.

In summary, we discussed the possibility of s -wave SC for Na_xCoO₂ based on a d - p model with a_{1g} -band and e'_g -bands, by considering EPI for breathing and shear phonons. The obtained T_c is strongly enhanced when shear phonons are taken into account, in addition to the breathing phonon. The estimated EPI for both phonons are large enough to realize s -wave SC against the strong Coulomb interaction in Na_xCoO₂. We find that T_c is still high even if small hole pockets are absent ($V_t \geq 0.6$), although the DOS at the Fermi level suddenly decreases to one-third of its value at $V_t \geq 0.6$. This enhancement of T_c is brought by the valence-band-SK mechanism due to shear phonons. In future, we will study the effect of Coulomb interaction to obtain a realistic T_c , and to explain the anisotropy of the superconducting gap.

We are grateful to M. Sato, Y. Kobayashi, K. Ishida, Y. Ihara, Y. Matsuda, T. Sato and T. Shimojima for valuable discussions on experiments. We also thank K. Yamada, D.S. Hirashima, Y. Tanaka, K. Kuroki, and authors of ref. [15] for useful comments and discussions.

-
- [1] M. Yokoi, T. Moyoshi, Y. Kobayashi, M. Soda, Y. Yasui, M. Sato and K. Kakurai: J. Phys. Soc. Jpn. **74** (2005) 3046.
 - [2] Y. Ihara, K. Ishida, K. Yoshimura, K. Takada, T. Sasaki, H. Sakurai and E. T. Muromachi: J. Phys. Soc. Jpn. **74** (2005) 2177.
 - [3] F. L. Ning, T. Imai: Phys. Rev. Lett. **94** (2005) 227004.
 - [4] Y. Kobayashi, H. Watanabe, M. Yokoi, T. Moyoshi, Y. Mori, and M. Sato: J. Phys. Soc. Jpn. **74** (2005) 1800.
 - [5] Y. Ihara, K. Ishida, H. Takeya, C. Michioka, M. Kato, Y. Itoh, K. Yoshimura, K. Takada, T. Sasaki, H. Sakurai and E.T. Muromachi: cond-mat/0511436.
 - [6] H.-B. Yang, Z.-H. Pan, A.K.P. Sekharan, T. Sato, S. Souma, T. Takahashi, R. Jin, B.C. Sales, D. Mandrus, A.V. Fedorov, Z. Wang, H. Ding: Phys. Rev. Lett. **95** (2005) 146401.
 - [7] M.Z. Hasan, D.Qian, Y. Li, A.V. Fedorov, Y.-D. Chuang, A.P. Kuprin, M.L. Foo, R.J. Cava: cond-mat/0501530.
 - [8] T. Shimojima, *et al*: unpublished
 - [9] D.J. Singh: Phys. Rev. B **61** (2000) 13397.
 - [10] M. Mochizuki, Y. Yanase and M. Ogata: J. Phys. Soc. Jpn. **74** (2005) 1670.
 - [11] K. Yada and H. Kontani: J. Phys. Soc. Jpn. **74** (2005) 2161.

- [12] D. Wu, J. L. Luo, and N. L. Wang: cond-mat/0501100.
- [13] S. Lupi, M. Ortolani, and P. Calvani: Phys. Rev. B **69** (2004) 180506(R).
- [14] K. Yada and H. Kontani: cond-mat/0507066.
- [15] Z. Li, J. Yang, J. G. Hou, and Q. Zhu: Phys. Rev. B **70** (2004) 144518.
- [16] K. Yada and H. Kontani: in preparation
- [17] W. A. Harrison: *Elementary Electronic Structure* (World Scientific, 1999, Singapore).
- [18] H. Kontani: Phys. Rev. B **70** (2004) 054507.
- [19] Y. Ihara, K. Ishida, C. Michioka, M. Kato, K. Yoshimura, K. Takada, T. Sasaki, H. Sakurai and E.T. Muromachi: J. Phys. Soc. Jpn. **74** (2005) 867.
- [20] Kazuhiko Kuroki, Seiichiro Onari, Yukio Tanaka, Ryotaro Arita, Takumi Nojima: cond-mat/0508482